miR-17 acts as a tumor suppressor by negatively regulating the miR-17-92 cluster

Yan Sweat,[1] Ryan J. Ries,[2] Mason Sweat,[1] Dan Su,[3,4] Fan Shao,[3,4] Steven Eliason,[3,4] and Brad A. Amendt[3,4,5]

[1]Harvard University, Boston, MA 02115, USA; [2]Weill-Cornell Medical College, Cornell University, New York, NY 10075, USA; [3]The University of Iowa, Department of Anatomy and Cell Biology, Iowa City, IA 52242, USA; [4]Craniofacial Anomalies Research Center, The University of Iowa, Iowa City, IA 52242, USA; [5]Iowa Institute for Oral Health Research, The University of Iowa, Iowa City, IA 52242, USA

Anaplastic thyroid cancer (ATC) is an aggressive, highly metastatic cancer that expresses high levels of the microRNA (miR)-17-92 cluster. We employ an miR inhibitor system to study the function of the different miRs within the miR-17-92 cluster based on seed sequence homology in the ATC SW579 cell line. While three of the four miR-17-92 families were oncogenic, we uncovered a novel role for miR-17 as a tumor suppressor in vitro and in vivo. Surprisingly, miR-17 inhibition increased expression of the miR-17-92 cluster and significantly increased the levels of the miR-18a and miR-19a mature miRs. miR-17 inhibition increased expression of the cell cycle activator CCND2, associated with increased cell proliferation and tumor growth in transplanted SW579 cells in xenograft mice. miR-17 regulates MYCN and c-MYC expression in SW579 cells, and the inhibition of miR-17 increased MYCN and c-MYC expression, which increased pri-miR-17-92 transcripts. Thus, inhibition of miR-17 activated the expression of the oncogenic miRs, miR-18a and miR-19a. While many cancers express high levels of miR-17, linking it with tumorigenesis, we demonstrate that miR-17 inhibition does not inhibit thyroid tumor growth in SW579 and MDA-T32 ATC cells but increases expression of the other miR-17-92 family members and genes to induce cancer progression.

INTRODUCTION

The miR-17-92 cluster, located on human chromosome 13, is a polycistronic cluster encoding six mature miRs: miR-17, miR-18a, miR-19a, miR-20a, miR-19b-1, and miR-92a-1. This highly conserved cluster has been shown to be expressed in many different murine tissues and is also expressed at high levels in embryonic stem cells during embryogenesis.[1–4] There are several paralogues of this cluster found in the human genome as well. Together, this cluster and its paralogues encode 15 mature miRs, which can be further divided into four different families (miR-17, miR-18, miR-19, and miR-92) based on seed sequence homology. The expression of the cluster has been demonstrated to be activated by c-MYC as well as by MYCN.[5–11] Furthermore, the over-expression of miR-17-92 was found to compensate for the inactivation of c-MYC and drive cancer cell proliferation in vivo and in vitro.[12] An oncogenic role for the miR-17-92 cluster has been reported in anaplastic thyroid cancer (ATC).[13]

In many cases, thyroid cancers are well-differentiated, slow-growing tumors that are easily treated by resection, and treatments result in high rates (∼85%) of disease-free survival in patients.[14–16] However, a small fraction of ATCs (3%) are derivatives of non-differentiated, rapidly proliferating, and highly metastatic cells. These cases of ATC have no currently approved treatment, and the mean survival time after a patient is diagnosed is just over 4 months. Only 5% of patients with ATC will survive longer than 5 years.[17,18] There is a desperate need to identify the molecular drivers of ATC and to develop therapeutics to combat ATC tumors and metastases.

Previous work aimed at uncovering the molecular underpinnings of ATC has utilized different cell lines obtained from ATC patients to discover oncogenes that drive tumor proliferation. Disruption of c-MYC, a member of the MYC family, which are commonly over-expressed genes in many cancer types, was shown to inhibit the proliferation of four distinct ATC cell lines, thus demonstrating its involvement in ATC progression[19].

In this study, we investigated inhibiting the miR-17-92 cluster using a plasmid-based miR inhibitor system (PMIS) to inhibit the individual miR families found within the cluster.[20,21] We became interested in ATC because our PMIS-miR-17-92 transgenic mice did not develop a thyroid gland.[20,21] Interestingly, while ATC SW579 cells expressing the inhibitors for miR-18a, miR-19a, and miR-92a-1 had decreased proliferation, the specific inhibition of miR-17 simulated growth. While conventional hypotheses would suggest that inhibiting the high levels of miR-17 expression in ATC cells would decrease proliferation and tumor formation, we report a new mechanism suggesting that miR-17 acts as a tumor suppressor. We further demonstrate that miR-17 regulates the expression of c-MYC and MYCN, and that inhibiting miR-17 results in increased expression of these factors driving high expression of the miR-17-92 cluster. Because many tumors and cancer cells have been profiled for miR expression and some tumors and cancers express high levels of miR-17, and in the
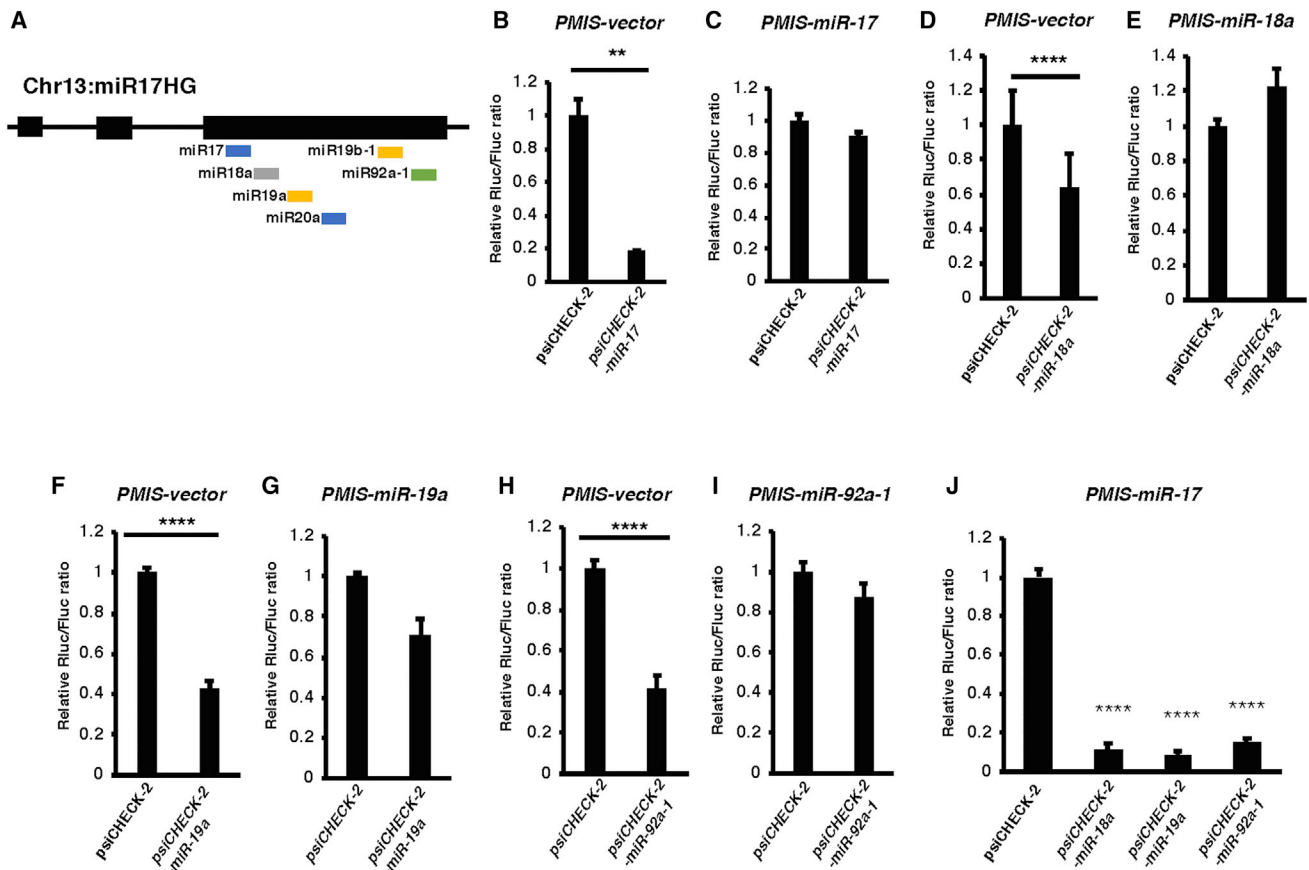
Figure 1. The PMIS inhibitor system inhibits *miR* activity in SW579 cells

(A) Schematic of the *miR-17-92* cluster in the human genome. The cluster is expressed as a single transcript that is then processed into six functional miRs with three different functional groups (color coded). (B and C) The control psiCHECK-2 reporter or the psiCHECK-2-*miR-17* reporter containing an *miR-17*-binding site were transfected into SW579 cells expressing PMIS vector or *PMIS-miR-17*. The *miR-17* reporter was repressed by endogenous *miR-17* activity in the PMIS-vector cell line but not in SW579 cells expressing the inhibitor to *miR-17* (*PMIS-miR-17*), demonstrating *miR-17* function was inhibited. (D and E) The experiment performed in (B) and (C) was repeated using a reporter containing the *miR-18a*-binding site and the stable SW579 cell line expressing *PMIS-miR-18a*. (F and G) The *miR-19a* reporter was assayed as in (B) and (C) and partially rescued in cells expressing *PMIS-miR-19a*. (H and I) The reporter containing a binding site for *miR-92a-1* in SW579 cells expressing *PMIS-vector* was rescued in SW579 cells expressing *PMIS-miR-92a-1*. (J) The activity of a control reporter was compared with the activity of reporters containing binding sites for *miR-17*, *miR-18a*, *miR-19a*, and *miR-92a-1* transfected in SW579 cells expressing *PMIS-miR-17* to demonstrate that *PMIS-miR-17* did not rescue the function of *miR-18a*, *miR-19a*, or *miR-92*. **p < 0.01; ***p < 0.005; ****p < 0.001 (N = 5–10).

ATC cells we tested with high levels of *miR-17*, inhibiting *miR-17* had an adverse effect on tumor formation and is a cautionary tale for miR inhibition used in therapeutic applications.

RESULTS

The PMIS system specifically inhibits each *miR* within the *miR-17-92* cluster

The *miR-17-92* cluster in human chromosome *13:miR17HG* is expressed as a single transcript that is then processed into six mature microRNAs (*miR-17*, *miR-18a*, *miR-19a*, *miR-20a*, *miR-19b*, and *miR-92*). *miR-17* and *miR-20a* have an identical seed region sequence, as do *miR-19a* and *miR-19b*, while *miR-18a* and *miR-92a-1* are unique (but encoded redundantly in other locations of the genome) (Figure 1A). The PMIS system can be used to specifically inhibit target miR function through seed sequence recognition.[20–23] In order to

inhibit the different *miRs* in the *miR-17-92* cluster, different PMIS constructs were designed to target the seed region of *miR-17*, *miR-18a*, *miR-19a*, and *miR-92a-1*, and stable cell lines were created by infecting SW579 with PMIS lentivirus constructs expressing GFP. As a control, we used the SW579 cell line expressing a PMIS empty vector, which does not inhibit miR function.

Luciferase reporters were constructed to measure the activity of the *miR-17-92* members by cloning their binding sites into the 3′ UTR of the psiCHECK-2 luciferase reporter. The SW579 cell line endogenously expresses the *miR-17-92* cluster and individual family members at high levels. The addition of the *miR-17*-binding site to the reporter resulted in an ∼90% reduction in normalized signal compared with a reporter lacking the *miR-17*-binding site (Figure 1B) in SW579 cells expressing the non-specific *PMIS-vector*. However, when the experiment was
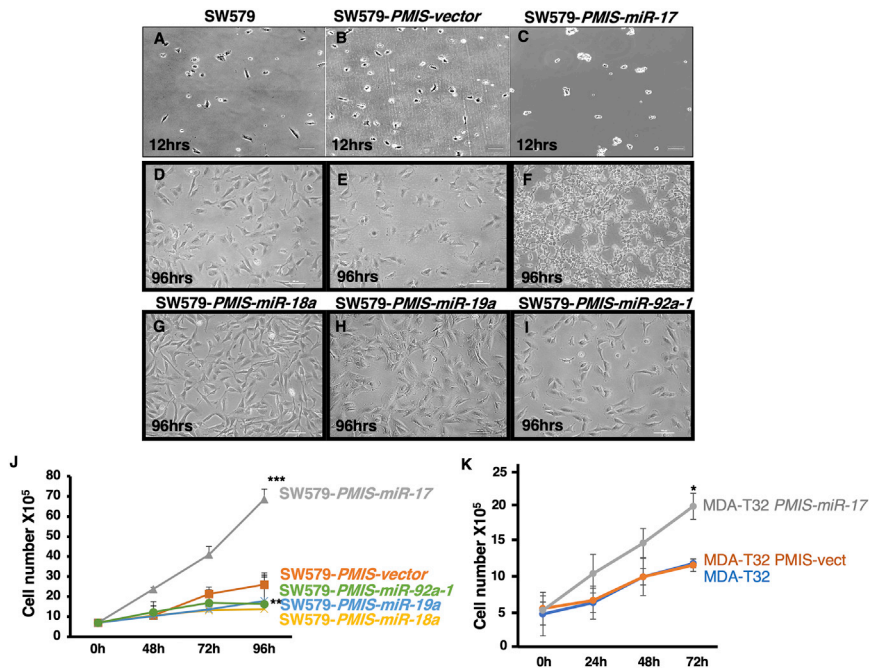
Figure 2. Inhibiting *miR-17* alters the morphology of SW579 cells

(A and D) The morphology of wild-type SW579 cells cultured in L-15 media after 12 h and 96 h, respectively. (B and E) The morphology of SW579 cells stably expressing the *PMIS-vector* construct after 12 h and 96 h, respectively. (C and F) SW579 cells transduced with and stably expressing *PMIS-miR-17*, after 12 h and 96 h, respectively, and these cells had an altered cell morphology growing in clusters. (G) A stable SW579 cell line expressing *PMIS-miR-18a*. (H) SW579 cells stably expressing *PMIS-miR-19a*. (I) An SW579 cell line stably expressing *PMIS-miR-92a-1*. (J) Cells stably expressing *PMIS-vector* or specific inhibitors for *miR-17*, *miR-18a*, *miR-19a*, and *miR-92a-1* were plated, and cell number was quantified after 48, 72, and 96 h. *PMIS-miR-17*-expressing cells proliferated significantly faster than the other cell lines. Cells expressing the *PMIS-miR-18a*, *PMIS-miR-19a*, and *PMIS-miR-92a-1* proliferated more slowly than cells expressing the control *PMIS-vector*. Cells are shown after 96 h of growth, and all cells were plated at 5×10^5. (K) The rate of proliferation of MDA-T32 cells was examined by plating wild-type cells and cells expressing either *PMIS-vector* or *PMIS-miR-17a* at 5×10^5 and counting cells at 24, 48, and 72 h *p < 0.05; **p < 0.01; ***p < 0.005 (N = 3–5).

repeated in SW579 expressing *PMIS-miR-17*, no significant loss in reporter activity was detected in the reporter with the *miR-17*-binding site (Figure 1C), demonstrating inhibition of *miR-17* function by the PMIS inhibitor.

The experiment was repeated to test the function of the other miRs found in the *miR-17-92* cluster. The luciferase signal obtained from transfecting each of the reporter constructs containing an miR-binding site was decreased in the cells expressing *PMIS-vector* only (Figures 1D, 1F, and 1H). However, in cell lines expressing PMIS inhibitor constructs targeting either *miR-18a*, *miR-19a*, or *miR-92a-1*, there was no decrease in reporter activity compared with a control luciferase construct lacking miR-binding sites (Figures 1E, 1G, and 1I). This demonstrates that the PMIS system can functionally inhibit each member of the *miR-17-92* cluster.

To determine if inhibiting *miR-17* affected the activity of other cluster members, we transfected the control reporter and reporters containing binding sites for other *miR-17-92* cluster members into SW579-*PMIS-miR-17* cells (Figure 1J). The biological activity of *miR-17* was inhibited in SW579-*PMIS-miR-17* cells, but the activities of the other *miRs* were unaffected, thus demonstrating the specificity of *PMIS-miR-17* for its target (Figures 1C and 1J). These data confirmed the specificity of the PMIS-miR-17-92 constructs as previously reported (20).

miR-17 inhibition in SW579 cells results in altered cell morphology, increased proliferation, and decreased migration

After confirming miR inhibition in each stable cell line, the morphology of each line was compared with the SW579 cells expressing the non-specific *PMIS-vector* (Figures 2A–2I). As a control for

growth, SW579, *SW579-PMIS-vector*, and *SW579-PMIS-miR-17* cells are shown after 12 h of growth (Figures 2A–2C). Cells expressing *PMIS-vector*, *PMIS-miR-18a*, *PMIS-miR-19a*, and *PMIS-miR-92a-1* had unaltered cellular morphology after 96 h in culture (Figures 2E, 2G, 2H, and 2I). However, *miR-17* inhibition altered the appearance of the SW579 cells, which had smaller somas and formed clusters after 96 h in culture (Figure 2F). These cells appear to be undifferentiated, similar to reports for the *miR-17-92* cluster in cancer stem cell biology.[24]

In order to determine if *miR-17-92* members regulated cell proliferation, equal cell numbers (7×10^5) were plated and the number of cells were measured at 48, 72, and 96 h (Figure 2J). The *miR-18a-*, *miR-19a-*, and *miR-92a-1*-inhibited cells proliferated at a slower rate than SW579 cells expressing *PMIS-vector*. However, the *PMIS-miR-17*-expressing cells proliferated approximately three times faster than the other cell types. It appears that the oncogenic function (proliferation) of the *miR-17-92* cluster was specific for the *miR-18*, *miR-19*, and *miR-92* families, while *miR-17* functions as a tumor cell growth suppressor.

To determine if the effect of inhibiting *miR-17* was specific for SW579 cells, we also generated an MDA-T32 papillary thyroid carcinoma cell line with stable expression of either *PMIS-vector* or *PMIS-miR-17*. Proliferation experiments revealed that inhibiting *miR-17* in MDA-T32 cells also resulted in increased cell proliferation, while the stable line expressing *PMIS-vector* had no difference in proliferation compared with parental cells (Figure 2K).

Because *miR-17* has been shown to target *BCL2L11* (*Bim*) and *PTEN*, we determined their expression in SW579 cells stably expressing
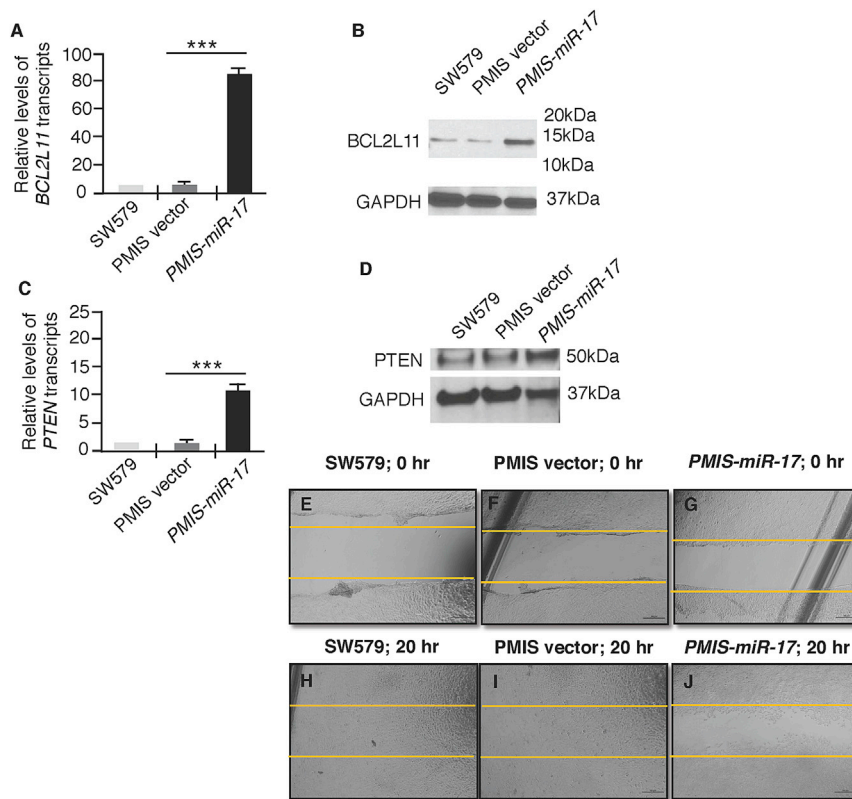
Figure 3. *miR-17* regulates *BIM*, *PTEN*, and cell migration

(A and B) *BCL2L11* transcripts and protein were increased in SW579 cells expressing the *PMIS-miR-17* inhibitor, respectively. (C and D) *PTEN* transcripts and protein were increased in SW579 cells expressing the *PMIS-miR-17* inhibitor, respectively. (E–G) SW579 cells, cells stably expressing the PMIS vector or *PMIS-miR-17* were grown to confluency and an approximately 2-cm scratch was made to remove cells, denoted by orange lines, respectively. (H–J) The cells as in (E)–(G) were visualized after 20 h for growth/migration into the cell-free area. ***$p < 0.005$ (N = 3).

PMIS-miR-17.[12,13,25–28] The inhibition of *miR-17* in SW579 cells up-regulated the expression of *BCL2L11* transcripts and protein levels compared with controls (Figures 3A and 3B). The inhibition of *miR-17* also increased *PTEN* transcripts and protein levels (Figures 3C and 3D). *miR-17* has been implicated in the regulation of cell migration in several tumor cell lines. To understand the effect of *miR-17* on cell migration, we removed an area of SW579 cells and measured their ability to migrate into the cell void region after 20 h in culture. The SW579 cells expressing the *PMIS-miR-17* inhibitor did not fill in the cell void area after 20 h, whereas the wild-type and control PMIS-vector cells completely migrated into the cell void area (Figures 3E–3J). Thus, the inhibition of *miR-17* in these cells inhibits cell migration. It is not clear how *PMIS-miR-17* SW579 cells can show increased proliferation, and decreased migration, although *Bim* has previously been demonstrated to act as a negative regulator of cell migration.[29] We have previously shown that *miR-17* inhibition increased Bim expression, which may decrease migration.[20] We speculate that these cells form clusters of undifferentiated cells (Figure 2C), similar to the role of the *miR-17-92* cluster in embryonic stem cells, and thus do not migrate as a monolayer of cells.[30]

To determine if the rapid proliferation phenotype observed in the *PMIS-miR-17* SW579 cell line was relevant *in vivo*, we injected these cells as well as the parental cells into immunocompromised *Foxn1^(nu/j)* mice and assayed for tumor growth (Figure 4). After 3 weeks, tumors derived from SW579 cells or S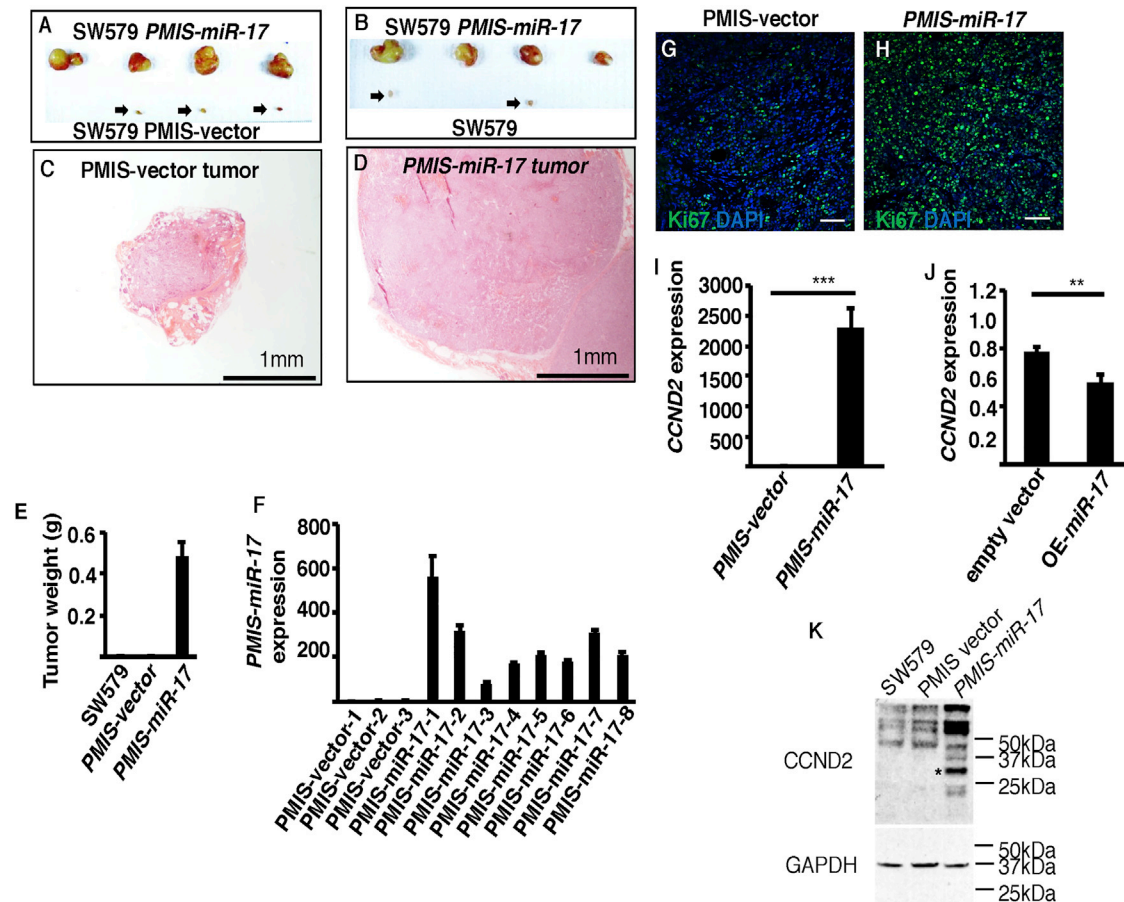W579 cells expressing *PMIS-vector* were small and not well formed (Figures 4A and 4B, arrows bottom row). However, tumors derived from the SW579 cell line expressing *PMIS-miR-17* had formed rapidly at this stage (Figures 4A and 4B, top row). Control and *PMIS-miR-17* SW579 tumors had similar morphology, with the *PMIS-miR-17* tumors being larger and denser (Figures 4C and 4D, respectively). Tumors derived from SW579 *PMIS-miR-17* cells had a mean weight of 0.5 g (Figure 4E), and RT-qPCR confirmed that these tumors had high expression levels of *PMIS-miR-17* (Figure 4F). Cell proliferation was assayed in *PMIS-vector* and *PMIS-miR-17* tumors by Ki67 staining, and the *PMIS-miR-17* tumors contained more proliferative cells than control tumors (Figures 4G and 4H).

Previous studies have demonstrated that Cyclin D2 (*CCND2*) is an *miR-17* target.[31] *CCND2* is required for cell cycle G1/S transition, and high levels of expression correlate with several tumors. Comparing *CCND2* expression in SW579 *PMIS-vector* cells and SW579 *PMIS-miR-17* cells revealed that inhibiting *miR-17* resulted in significantly increased expression of *CCND2* (Figure 4I). Conversely, over-expression of *miR-17* resulted in a decrease in *CCND2* transcripts (Figure 4J). Western blot analyses demonstrated an increase in CCND2 protein expression when *miR-17* was inhibited by *PMIS-miR-17* (asterisk, Figure 4K).

miR-17 expression negatively regulates expression of the other cluster members

We were surprised by the *in vivo* results showing that inhibition of *miR-17* increased tumor growth. It has been suggested that high expression of *miR-17* causes tumors and has been used as a biomarker for cancer.[24] However, it has also been shown that other *miR-17-92* family members are associated with cancer progression.[12,13,25–28] To determine if other miRs in the *miR-17-92* cluster were increased by inhibition of *miR-17*, primers were designed to probe different regions of *pri-miR-17-92* cluster transcript (Figure 5A).[30] Interestingly, in SW579 cells expressing *PMIS-miR-17*, greater amounts of the *pri-miR-17-92* cluster were detected by each of the primer sets designed to

Figure 4. Inhibiting *miR-17* results in increased tumorigenesis in xenograft nude mice

(A) NU/J mice were injected on each flank with either SW579 cells expressing *PMIS-vector* or *PMIS-miR-17*. After 3 weeks, the animals were euthanized, and the tumors were harvested (arrows denote control tumors). (B) Similar to (A), but the parental SW579 cell line was injected as a control (arrows denote control tumors). Overall, eight SW579 *PMIS-miR-17* tumors were analyzed (A and B). (C) H&E staining for sections from SW579 PMIS-vector tumor. (D) H&E staining for sections from SW579 *PMIS-miR-17* tumor. (E) Average tumor weight after 3 weeks. (F) RT-qPCR was used to detect *PMIS-miR-17* expression in the isolated tumors. (G and H) Ki67 staining in sections from SW579 PMIS-vector (G) and SW579-*PMIS-miR-17* (H) tumors (N = 4). (I) RT-qPCR was used to measure levels of the *CCND2* mRNA in *PMIS-vector* and *PMIS-miR-17* SW579 cell lines. ***$p < 0.005$ (N = 3). (J) The expression of *CCND2* upon over-expression of *miR-17* (OE-*miR-17*) on the mRNA level was analyzed with specific primers for *CCND2* by qPCR. Expression is shown as fold change compared with the empty vector control. Error bars represent the standard deviation from three experiments. The p values have been calculated by two-tailed t test. **$p < 0.01$; ***$p < 0.005$ (N = 3). (K) Western blot of CCND2 in SW579 cells, expressing the PMIS vector and *PMIS-miR-17*, asterisk (*) denotes CCND2 protein. GAPDH is used as a loading control and the CCND2 blot was stripped and re-probed for GAPDH.

measure its expression (Figure 5B), which indicates that *miR-17* regulates the transcription of the pri-*miR-17-92* cluster. Furthermore, inhibiting the activity of *miR-17* results in a higher expression of mature *miR-18a* and *miR-19a* as well as *miR-92a* (Figure 5C).

In order to determine if the upregulation of the *miR-17-92* cluster depended on the biological activity of *miR-17*, or if it was also linked with other cluster members, we examined levels of mature miRs in SW579 cells expressing inhibitors for either *PMIS-miR-18a*, *PMIS-miR-19a*, or *PMIS-miR92a-1* (Figures 5D–5F). Interestingly, in these other cell lines, the expression of the *miR-17-92* cluster was not increased, and we observed a reduction in the miR targeted by the PMIS inhibitor system, as we have previously reported.[20] However,

inhibition of *miR-18a* also decreased *miR-19a* levels (Figure 5D), but inhibition of *miR-19a* did not affect the levels of mature *miR-18a* (Figure 5E). We have previously shown using luciferase assays and binding sites for each miR that inhibition of *miR-18a* did not affect *miR-19a* binding, activity, or function.[20,21] Thus, *miR-18a* inhibition appears to affect the processing of *miR-19a* and this may influence tumor growth and progression. The inhibition of *miR-92a* (*PMIS-miR-92a-1*) did not affect the levels of the other mature miRs in the cluster (Figure 5F).

MYCN is regulated by *miR-17* in SW579 cells

The *miR-17-92* cluster is a well-established oncogene and has been shown to act downstream of MYCN in different cancer types.[8,9] Since
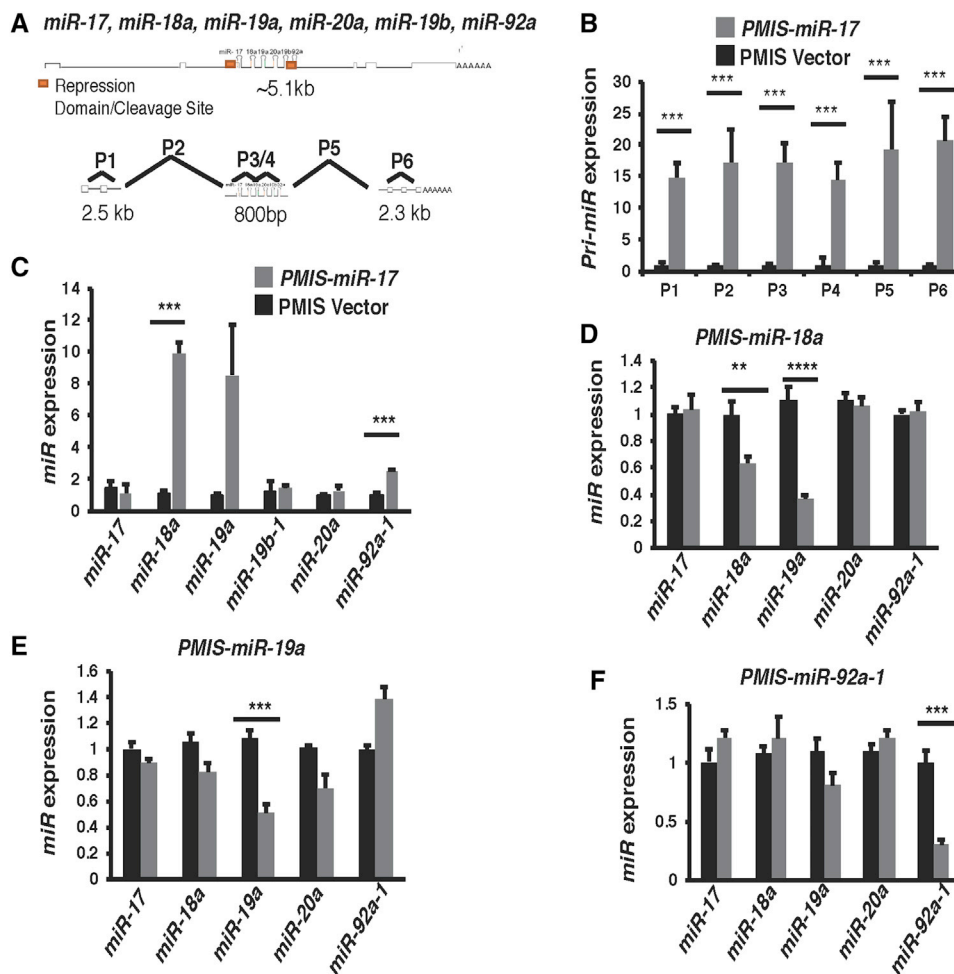
**Figure 5. The inhibition of *miR-17* regulates *miR-17-92* expression**

(A) A schematic of the primer sets used to detect different regions of the *pri-miR-17-92* cluster transcript. The two repression domains identified by Du et al.[30] are shown in the *pri-miR-17-92* transcript. (B) When *pri-miR-17-92* expression was measured with RT-qPCR in *PMIS-vector* cells (black) and *PMIS-miR-17-92* SW579 cells, the levels of *pri-miR* expression were greatly increased in the *miR-17* inhibitor cell line as shown by each primer set. ***p < 0.005 (N = 4). (C) Using RT-qPCR to measure the levels of the mature *miRs* processed from the *pri-miR-17-92* cluster in *PMIS-vector* cells (black bars) and *PMIS-miR-17* SW579 cells (gray bars) revealed that the mature levels of each miR were increased in the inhibitor cell line. ***p < 0.005 (N = 4). (D–F) Levels of the mature *miRs* encoded by the cluster were examined in SW579 cells expressing PMIS constructs inhibiting *miR-18a*, *miR-19a*, and *miR-92a-1*, respectively. Inhibiting these other *miRs* did not increase *pri-miR-17-92* cluster expression but resulted in decreased levels of the target *miR*. **p < 0.01; ***p < 0.005 (N = 4).

transcription of the *miR-17-92* cluster is increased when the function of *miR-17* is inhibited in SW579 cells, we hypothesized that *MYCN* expression would be increased as well. To test if *MYCN* was increased in SW579-*PMIS-miR-17* cells, *MYCN* transcript levels were detected using RT-qPCR in *PMIS-vector* and *PMIS-miR-17*-expressing SW579 cells. *MYCN* was increased in the *PMIS-miR-17* SW579 cells (Figure 6A). MYCN protein levels were also increased in SW579 cells expressing the *PMIS-miR-17* inhibitor (Figure 6B). The proto-oncogene, *c-MYC* is activated in different tumors,[32] and it appears that the *miR-17-92* cluster and *miR-17* inhibition regulates *c-MYC* transcripts and protein levels (Figures 6C and 6D). Furthermore, MYNC and c-MYC are known to activate expression of the *miR-17-92* cluster.[9]

RNA sequencing (RNA-seq) experiments (three biological replicates, N = 3) revealed a known link between *Collagen* genes and *Matrix Metalloproteases* (*MMPs*) as well as *thrombospondin-1* (*THBS-1*) and *thrombospondin-2* (*THBS-2*) genes in cancer and are increased in SW579 cells expressing *PMIS-miR-17* (Figure 6E). The RNA-seq data reveal multiple levels of thyroid cancer cell gene expression associated with thyroid tumors and now linked with *miR-17* inhibition.

Mechanisms of *miR-17* are similar in the papillary thyroid carcinoma MDA-T32 cell line

While we make no claim that all thyroid tumors will respond to *miR-17* inhibition the same as the SW579 cells, we tested the role of *miR-17* in the thyroid carcinoma MDA-T32 cell line, which we showed had
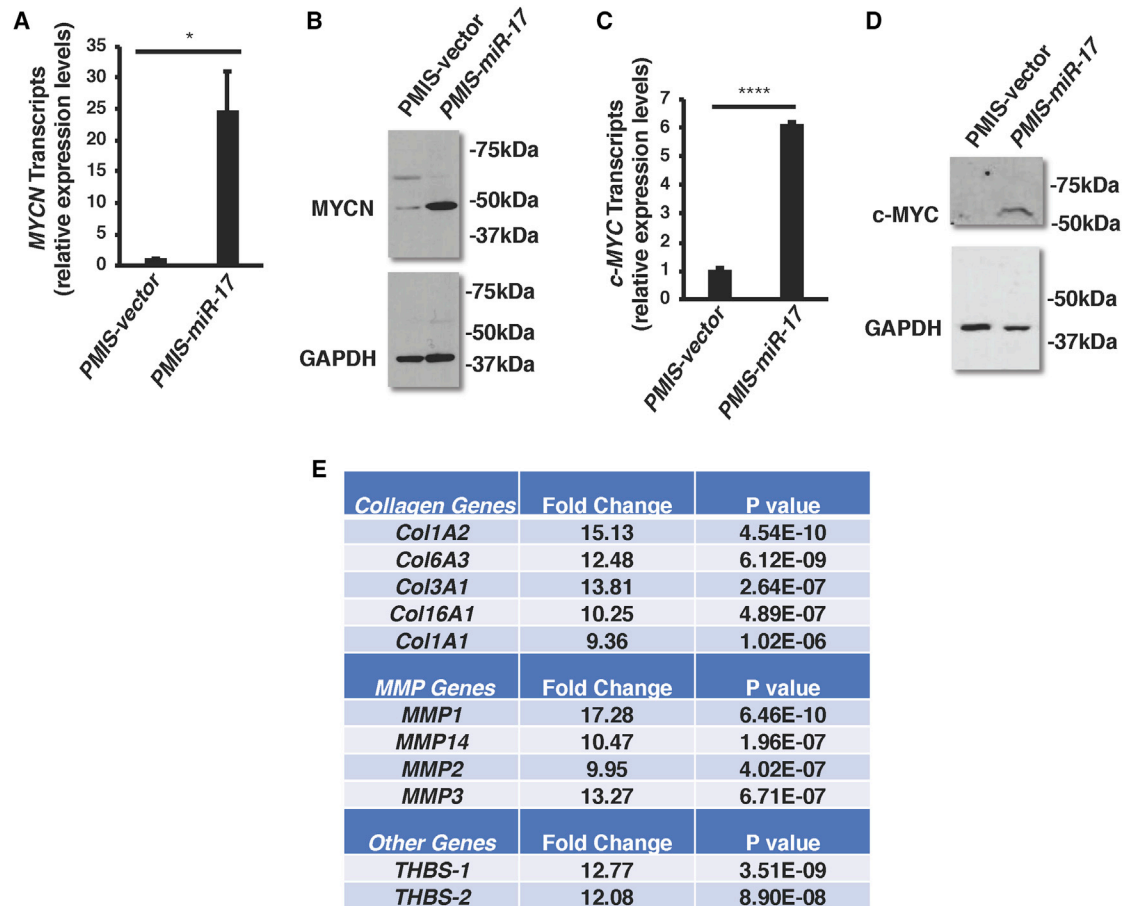
Figure 6. miR-17 regulates MYCN and c-MYC expression in SW579 cells

(A and B) MYCN transcripts and protein were increased in SW579 cells expressing the PMIS-miR-17 inhibitor, respectively. *p < 0.05 (N = 3). (C and D) c-MYC transcripts and protein were increased in SW579 cells expressing the PMIS-miR-17 inhibitor, respectively. ****p < 0.001 (N = 4). (E) Selected data from RNA-seq experiments showing an increase in gene expression of Collagen genes, MMP genes, and THBS genes in PMIS-miR-17 SW579 cells (N = 3).

increased proliferation upon inhibition of miR-17 (Figure 2H). The MDA-T32 cell line expresses miR-17 measured by luciferase activity (Figure 7A) as shown for the SW579 cell line. The biological activity of miR-17 was inhibited in MDA-T32-PMIS-miR-17 cells, but the activities of the other miRs were unaffected, thus demonstrating the specificity of PMIS-miR-17 for its target (Figure 7B), also shown for SW579 cells (Figure 1J). In addition, inhibiting the activity of miR-17 results in a higher expression of mature miR-18a and miR-19a as well as miR-92a (Figure 7C), also correlating with SW579 cells (Figure 5C). Lastly, both MYC and MYCN transcripts are increased upon miR-17 inhibition in MDA-T32 cells (Figure 7D), as in SW579 cells (Figures 6A and 6C). In both thyroid cancer cell lines, the mechanisms of miR-17 expression and regulation appear similar.

The PMIS-miR-17 inhibitor binds miR-17 with a high affinity, and the resulting complex of the inhibitor and the miR is very stable. Thus, when miR-17 levels are determined by qPCR in the presence of the inhibitor, they appear to be only reduced 50%. This is due to the mature miR-17 complexed to the inhibitor and released when the cells are lysed. However, the luciferase reporter assays demonstrate that the PMIS-miR-17 inhibitor effectively inhibits 90% of miR-17 activity.

DISCUSSION

Investigating the function of individual miRs within the miR-17-92 cluster reveals specific alternate functions for miR-17 versus other cluster members

Previous studies have examined the role of the miR-17-92 cluster in different types of cancer, including thyroid cancer,[3,8,13,33–35] and have shown that the cluster is an oncogene. These previous studies relied upon either the over-expression of the cluster as a whole or the inhibition of the miRs produced by the cluster. In this study, we adopted a new technology that offers the advantage of specifically inhibiting individual miRs within the cluster, and using cells that stably express miR inhibitors re-affirmed the findings of previous studies that have demonstrated the oncogenic role of miR-18a, miR-19a, and miR-92a-1, but not miR-17.
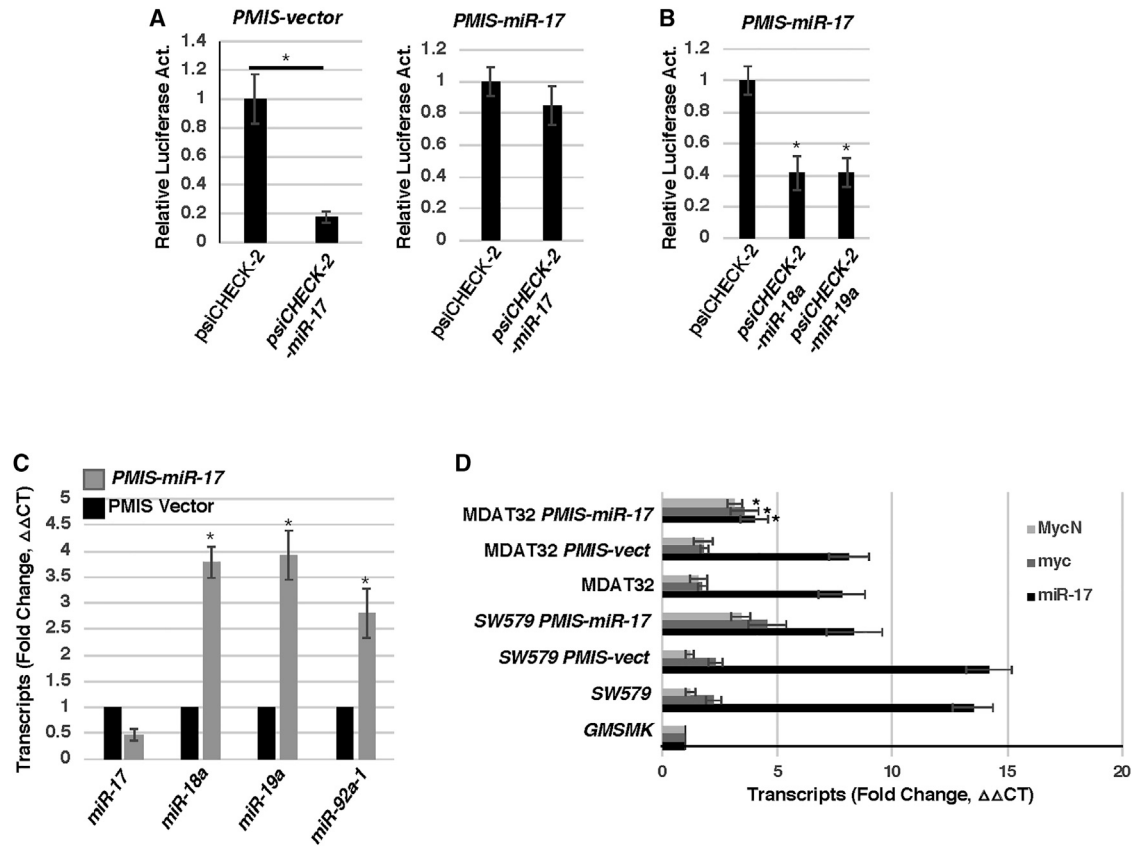
Figure 7. miR-17 inhibition increases *miR-18a*, *miR-19a*, *miR-92a-1*, *c-MYC*, and *MYCN* in MDA-T32 cells

(A) The control psiCHECK-2 reporter or the psiCHECK-2-*miR-17* reporter containing an *miR-17*-binding site were transfected into MDA-T32 cells expressing PMIS vector or *PMIS-miR-17*. The *miR-17* reporter was repressed by endogenous *miR-17* activity in the PMIS-vector cell line but not in MDA-T32 cells expressing the inhibitor to *miR-17* (*PMIS-miR-17*), demonstrating *miR-17* function was inhibited. (B) The activity of a control reporter was compared with the activity of reporters containing binding sites for *miR-18a* and *miR-19a* transfected in MDA-T32 cells expressing *PMIS-miR-17* to demonstrate that *PMIS-miR-17* did not rescue the function of *miR-18a* or *miR-19a*. (C) Using RT-qPCR to measure the levels of the mature *miRs* processed from the *pri-miR-17-92* cluster in *PMIS-vector* cells (black bars) and *PMIS-miR-17* MDA-T32 cells (gray bars) revealed that the mature levels of each miR were increased in the inhibitor cell line. (D) *MYCN* and *c-MYC* transcripts were increased in SW579 and MDA-T32 cells expressing the *PMIS-miR-17* inhibitor. Expression was normalized to a non-oncogenic GMSMK human oral epithelial cell line. *$p < 0.05$ (N = 3).

Interestingly, while the inhibition of the *miR-18*, *miR-19*, and *miR-92* families in SW579 cells resulted in the reduction of cell proliferation compared with the control, inhibiting *miR-17* in SW579 cells had the opposite effect. *PMIS-miR-17* SW579 cells had altered morphologies and proliferated rapidly when maintained *in vitro* as well as forming large tumors when they were injected into nude mice. The *PMIS-miR-17* SW579 cell line established rapidly growing tumors compared with wild-type SW579 cells and SW579 cells expressing the non-specific PMIS vector. Upon examination, the number of proliferative cells in tumors derived from *PMIS-miR-17* SW579 cells was increased compared with control tumors.

Taken together, these data indicate that the role for *miR-17* is distinct from the other families represented by the *miR-17-92* cluster in ATC. This finding differs from the results of a previous group that showed *miR-17* is oncogenic in ATC[13]; this group used a different ARO cell line, and it is possible that SW579 cells are controlled by a different

gene regulatory network. However, they also did not use cells stably expressing the *PMIS-miR-17* inhibitor, which allows for the dissection of miR function. Similarly, we also demonstrate that the inhibition of *miR-17* in MDA-T32 cells results in increased cell proliferation. Interestingly, these cells express high levels of endogenous *miR-17* and we show that *miR-17* targets CCND2, decreasing cell proliferation. Over-expression of *miR-17* by plasmid DNA in SW579 cells had a significant but small effect on *CCND2* transcript levels. Furthermore, over-expression of *miR-17* in a background of high endogenous *miR-17* expression had little effect on cell morphology and proliferation. However, using our system, we found that the upregulation of *miR-17* in the ATC lines does not correlate with increased oncogenic function.

The biogenesis of miRs from the *pri-miR-17-92* transcript

The *miR-17-92* cluster is also regulated by specific *cis*-acting sequences within the *pri-miR-17-92* transcript.[30] Two complementary repression
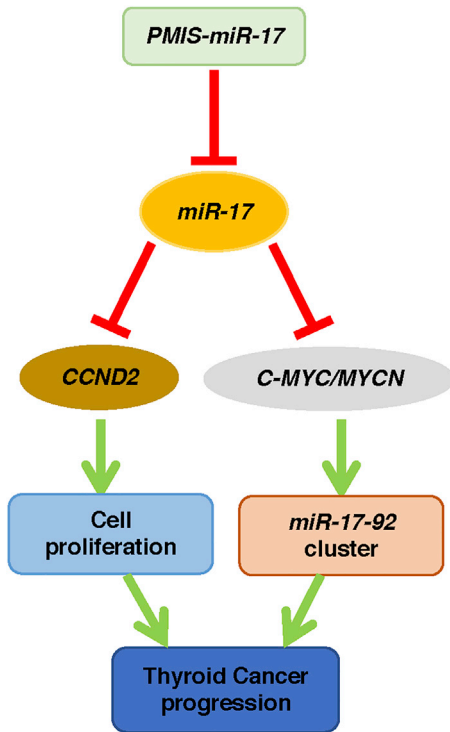
Figure 8. *miR-17* acts as a rheostat to regulate the expression of the *miR-17-92* cluster in ATC cells

Overall, using *PMIS-miR-17* inhibits the activity of *miR-17*, causing the decrease expression of *miR-17* and, concurrently, an increase in *CCND2*, *c-MYC*, and *MYCN*. The increase in c-MYC and MYCN then directly stimulates *miR-17-92* cluster expression and the other oncogenic miRs drive tumor growth.

domains (RDs) are located in the *pri-miR-17-92* transcript (shown in Figure 5A).[30] These two domains may interact to form a compact RNA structure that regulates or represses the processing of the *pri-miR-17-92* transcript except for *miR-92*. Furthermore, the 5′ flanking RD inhibits production of most miRs except for *miR-92*.[30] Interestingly, inhibition of *miR-17* in SW579 cells decreases mature *miR-17* levels but increases mature *miR-18a* and *miR-19a* levels, while *miR-19b* and *miR-20a* are unaffected. We speculate that *miR-17* may be involved in the processing of the *pri-miR-17-92* cluster.[30] *miR-17* could be regulating processing factors or interacting with sequences within the *pri-miR-17-92* transcript. More detailed experiments are required to determine if *miR-17* interacts with the *pri-miR-17-92* transcript.

The expression of *miR-17* driven by c-MYC and MYCN forms a negative feedback loop

Upon inhibiting *miR-17* in SW579 cells, the oncogene *MYCN* was found to be highly upregulated both transcriptionally and translationally, while the over-expression of *miR-17* resulted in a decrease of *MYCN* transcripts. Furthermore, *c-MYC* (a proto-oncogene) expression was also found to be increased when *miR-17* was inhibited in SW579 cells. Both *MYCN* and *c-MYC* are known targets of *miR-17* and are associated with tumorigenesis.

c-MYC and MYCN have been shown to bind directly to the promoter sequence of the *miR-17-92* cluster,[8,9,36] and, indeed, the expression of the cluster is highly upregulated in *PMIS-miR-17*-expressing cells. Therefore, high levels of *miR-17* act to decrease *c-MYC* and *MYCN* levels which reduce activation of the *miR-17-92* cluster. This feedback loop regulates the levels of the oncogenes and the *miR-17-92* cluster. However, other factors and mechanisms also regulate *miR-17-92* levels, including NOTCH signaling, which is activated at higher levels in thyroid cancer.[37] These other mechanisms contribute to increased expression of the *miR-17-92* cluster and the oncogenic effects of *miR-18a*, *miR-19a*, and *miR-92a-1*.

We have uncovered a new mechanism by which *miR-17* regulates the expression of the entire *miR-17-92* cluster by regulating transcription factors promoting cluster expression (Figure 8). We show that inhibition of *miR-17* increases *CCND2*, *c-MYC*, and *MYNC* expression, which activates cell proliferation, and *miR-17-92* expression, which leads to thyroid tumor progression (Figure 8). In addition, *miR-17* may play a role in the processing of the *pri-miR-17-92* transcript to pre-miRs. This novel regulatory scheme might be utilized by other miR clusters as well.

miR-17 expression appears to negatively regulate thyroid tumor growth

This work clearly demonstrates that the *miR-17* family plays a tumor suppressor role in at least two ATC models by negatively regulating the expression of *MYCN*, *c-MYC*, and other oncogenic miRs found in the *miR-17-92* cluster. The identification and use of miRs as biomarkers for diseases such as cancer are valuable; however, using miR expression levels to design therapeutic treatments must be carefully analyzed prior to treatments. Effective treatments for ATC are required, and currently there are few options.[18] The data shown in these studies demonstrate that inhibiting an miR whose high expression is associated with cancer can have deleterious effects. Furthermore, the PMIS can determine the role of each miR within a cluster and by inhibiting *miR-17* we demonstrate an increase in thyroid tumorigenesis. Therefore, inhibiting *miR-17* does not appear to be a therapeutic response as a treatment for ATC.

MATERIALS AND METHODS
Animals
Animals were housed with the Program of Animal Resources at the University of Iowa, and the procedures followed guidelines determined by the University of Iowa Institutional Care and Use Committee. Nude mice (*Foxn1*[nu/j]) were obtained from Jackson Laboratories (stock number 002019) for tumor studies.

Construction of stable cell lines expressing PMIS inhibitor molecules

To establish stable cell lines, we used PMIS inhibitor plasmids *PMIS-miR-17*, *PMIS-miR-18a*, *PMIS-miR-19a*, and *PMIS-miR-92a-1*, and the construction of these vectors has been previously described.[20] To produce lentivirus, 100-mm dishes of HEK293FT cells were transfected with a mix of psPAX2, pMD2.G, and the desired inhibitor

construct using PEI (3:1 PEI:DNA ratio). After 48 h, cells and media containing the virus were harvested. Cells were pelleted and lysed and the filtered supernatant was used to infect ATC SW579 and MDA-T32 cells. Both cell lines were successfully transduced and expressed the PMIS inhibitor construct and GFP several days after infection. These cells were purified by fluorescence-activated cell sorting (FACS) sorting and puromycin (1 μg/mL) selection and maintained in L-15 medium according to the American Type Culture Collection (ATCC) protocol. MDA-T32 cells (ATCC, CRL3351) were cultured in RPMI with 10% FBS serum.

Proliferation and migration assays

Control and cells expressing the different PMIS inhibitor constructs were plated in equal amounts (7×10^5 cells) in 60-mm dishes and, at the given timepoints, were trypsinized and counted using a hemocytometer. Cells were plated at high density and a scratch was made in the ~80% confluent cells using a sterile 200-μL pipette tip, the cells were washed twice in media to remove free cells and cell debris, and photos were taken at time 0 and after 20 h. Scratch photos were analyzed by ImageJ and the closure distance of the scratch was calculated. Cell proliferation assays started with 5×10^5 cells at 0 h and cell proliferation measured by cell counting at 24 h, 48 h, and 72 h for MDA-T32 cells and 96 h for SW579 cells.

Tumor injections

To form solid tumors (5×10^6), cancer cells were injected subcutaneously in the flanks of NU/J mice. After 3 weeks, tumors expressing *PMIS-miR-17* reached a critical size and the experiment was stopped by euthanizing the mice. Tumors were collected, weighed, and prepared for RNA, protein, and tissue sections for analysis by qPCR, western blot, and immunofluorescence, respectively.

RT-qPCR

RNA was isolated using the Qiagen miRNA-easy kit and protocol. RNA quality was assessed by gel electrophoresis. Reverse transcription for mRNA used the Takara RT kit (RR036A-1). Reverse transcription for miRNA used the Qiagen miScript II RT Kit (catalog no. 218161). Quantitative PCR reactions were performed using the Takara TB Green Premix Ex Taq (RR420L).

Western blotting

Protein was isolated from cells by lysing with reporter lysis buffer (Promega E397A). Protein concentration was measured using the Bradford assay, 0 μg of protein was loaded per well, and 10%–12% SDS-polyacrylamide gels were cast. After running the gel, gels were transferred to polyvinylidene fluoride (PVDF) and blocked for 1 h at room temperature (RT) using 5% milk. After blocking, primary antibody was applied overnight at 4°C. Membranes were washed three times using 1× PBST (Phosphate buffered saline with Tween) and the secondary antibody was applied in milk (1:10,000) for 1 h at RT. Membranes were washed three times using 1× PBST and primed for development using enhanced chemiluminescence (ECL). In some experiments, the blots were stripped and re-probed for glyceraldehyde 3-phosphate dehydrogenase (GAPDH); in others, duplicate samples were run side by side on the same gel, transferred to PVDF membranes, cut in half, and probed separately for each protein.

Immunofluorescence assays

Approximately 7-μm sections were cut from paraffin-embedded samples and attached to slides by baking for several hours. After attachment, sections were de-paraffinized with two changes of xylene and rehydrated through a reverse ethanol gradient. Antigen retrieval was performed by placing the slides in a chamber containing citrate buffer and placing the chamber in a flask of boiling water for 20 min. After antigen retrieval, slides were allowed to cool to RT over several hours, permeabilized with PBST, washed twice with PBS, and blocked with 20% donkey serum for 1 h at RT. After blocking, primary antibody was incubated with the sections overnight at 4°C. Slides were then washed three times in PBS, and incubated with secondary antibody for 1 h at RT. After washing three times, slides were incubated with DAPI solution for 10 min at RT.

Statistical analysis

For each condition, at least three experiments were performed and the results are presented as the mean ± SEM. The differences between two groups of conditions were analyzed using an independent, two-tailed t test.

AUTHOR CONTRIBUTIONS

Y.S. designed and performed experiments, analyzed data, prepared figures, wrote draft of manuscript, and edited the manuscript. R.J.R. designed and performed experiments, analyzed data, prepared figures, and edited the manuscript. M.S. performed experiments, analyzed data, and edited the manuscript. D.S. designed and performed experiments, analyzed data, prepared figures, and edited the manuscript. F.S. performed experiments and analyzed data. S.E. designed and performed experiments, analyzed data, prepared figures, and edited the manuscript. B.A.A. designed and performed experiments, analyzed data, prepared figures, and wrote and edited the manuscript.

DECLARATION OF INTERESTS

B.A.A. is the owner and Chief Scientific Officer of NaturemiRI, and PMIS microRNA inhibitors.

REFERENCES

1. Tanzer, A., and Stadler, P.F. (2004). Molecular evolution of a microRNA cluster. J. Mol. Biol. *339*, 327–335.

2. Vidigal, J.A., and Ventura, A. (2012). Embryonic stem cell miRNAs and their roles in development and disease. Semin. Cancer Biol. *22*, 428–436.

3. Concepcion, C.P., Bonetti, C., and Ventura, A. (2012). The microRNA-17-92 family of microRNA clusters in development and disease. Cancer J. *18*, 262–267.

4. Ventura, A., Young, A.G., Winslow, M.M., Lintault, L., Meissner, A., Erkeland, S.J., Newman, J., Bronson, R.T., Crowley, D., Stone, J.R., et al. (2008). Targeted deletion reveals essential and overlapping functions of the miR-17w92 family of miRNA clusters. Cell *132*, 875–886.

5. Dews, M., Fox, J.L., Hultine, S., Sundaram, P., Wang, W., Liu, Y.Y., Furth, E., Enders, G.H., El-Deiry, W., Schelter, J.M., et al. (2010). The myc-miR-17∼92 axis blunts TGFβ signaling and production of multiple TGFβ-dependent antiangiogenic factors. Cancer Res. *70*, 8233–8246.

6. Dews, M., Homayouni, A., Yu, D., Murphy, D., Sevignani, C., Wentzel, E., Furth, E.E., Lee, W.M., Enders, G.H., Mendell, J.T., et al. (2006). Augmentation of tumor angiogenesis by a Myc-activated microRNA cluster. Nat. Genet. *38*, 1060–1065.

7. Fontana, L., Fiori, M.E., Albini, S., Cifaldi, L., Giovinazzi, S., Forloni, M., Boldrini, R., Donfrancesco, A., Federici, V., Giacomini, P., et al. (2008). Antagomir-17-5p abolishes the growth of therapy-resistant neuroblastoma through p21 and BIM. PLoS ONE *3*, e2236.

8. Mestdagh, P., Fredlund, E., Pattyn, F., Schulte, J.H., Muth, D., Vermeulen, J., Kumps, C., Schlierf, S., De Preter, K., Van Roy, N., et al. (2010). MYCN/c-MYC-induced microRNAs repress coding gene networks associated with poor outcome in MYCN/c-MYC-activated tumors. Oncogene *29*, 1394–1404.

9. O'Donnell, K.A., Wentzel, E.A., Zeller, K.I., Dang, C.V., and Mendell, J.T. (2005). c-Myc-regulated microRNAs modulate E2F1 expression. Nature *435*, 839–843.

10. Sylvestre, Y., De Guire, V., Querido, E., Mukhopadhyay, U.K., Bourdeau, V., Major, F., Ferbeyre, G., and Chartrand, P. (2007). An E2F/miR-20a autoregulatory feedback loop. J. Biol. Chem. *282*, 2135–2143.

11. Woods, K., Thomson, M.J., and Hammond, S.M. (2007). Direct regulation of an oncogenic micro-RNA cluster by E2F transcription factors. J. Biol. Chem. *282*, 2130–2134.

12. Li, Y., Choi, P.S., Casey, S.C., Dill, D.L., and Felsher, D.W. (2014). MYC through miR-17-92 suppresses specific target genes to maintain survival, autonomous proliferation, and a neoplastic state. Cancer Cell *26*, 262–272.

13. Takakura, S., Mitsutake, N., Nakashima, M., Namba, H., Saenko, V.A., Rogounovitch, T.I., Nakazawa, Y., Hayashi, T., Ohtsuru, A., and Yamashita, S. (2008). Oncogenic role of miR-17-92 cluster in anaplastic thyroid cancer cells. Cancer Sci. *99*, 1147–1154.

14. Weinberger, P., Ponny, S.R., Xu, H., Bai, S., Smallridge, R., Copland, J., and Sharma, A. (2017). Cell cycle M-phase genes are highly upregulated in anaplastic thyroid carcinoma. Thyroid *27*, 236–252.

15. Manzella, L., Stella, S., Pennisi, M.S., Tirrò, E., Massimino, M., Romano, C., Puma, A., Tavarelli, M., and Vigneri, P. (2017). New insights in thyroid cancer and p53 family proteins. Int. J. Mol. Sci. *18*, 1325.

16. Yu, Y., Dong, L., Li, D., Chuai, S., Wu, Z., Zheng, X., Cheng, Y., Han, L., Yu, J., and Gao, M. (2015). Targeted DNA sequencing detects mutations related to susceptibility among familial non-medullary thyroid cancer. Sci. Rep. *5*, 16129.

17. Nagaiah, G., Hossain, A., Mooney, C.J., Parmentier, J., and Remick, S.C. (2011). Anaplastic thyroid cancer: a review of epidemiology, pathogenesis, and treatment. J. Oncol. *2011*, 542358.

18. Saini, S., Tulla, K., Maker, A.V., Burman, K.D., and Prabhakar, B.S. (2018). Therapeutic advances in anaplastic thyroid cancer: a current perspective. Mol. Cancer *17*, 154.

19. Enomoto, K., Zhu, X., Park, S., Zhao, L., Zhu, Y.J., Willingham, M.C., Qi, J., Copland, J.A., Meltzer, P., and Cheng, S.Y. (2017). Targeting MYC as a therapeutic intervention for anaplastic thyroid cancer. J. Clin. Endocrinol. Metab. *102*, 2268–2280.

20. Cao, H., Yu, W., Li, X., Wang, J., Gao, S., Holton, N.E., Eliason, S., Sharp, T., and Amendt, B.A. (2016). A new plasmid-based microRNA inhibitor system that inhibits microRNA families in transgenic mice and cells: a potential new therapeutic reagent. Gene Ther. *23*, 527–542.

21. Ries, R.J., Yu, W., Holton, N., Cao, H., and Amendt, B.A. (2017). Inhibition of the miR-17-92 cluster separates stages of palatogenesis. J. Dent. Res. *96*, 1257–1264.

22. Sweat, M., Sweat, Y., Yu, W., Su, D., Leonard, R.J., Eliason, S.L., and Amendt, B.A. (2021). The miR-200 family is required for ectodermal organ development through the regulation of the epithelial stem cell niche. Stem Cells *39*, 761–775.

23. Eliason, S., Sharp, T., Sweat, M., Sweat, Y.Y., and Amendt, B.A. (2020). Ectodermal organ development is regulated by a microRNA-26b-Lef-1-Wnt signaling axis. Front Physiol. *11*, 780.

24. Fuziwara, C.S., and Kimura, E.T. (2015). Insights into regulation of the miR-17-92 cluster of miRNAs in cancer. Front Med. *2*, 64.

25. Mu, P., Han, Y.C., Betel, D., Yao, E., Squatrito, M., Ogrodowski, P., de Stanchina, E., D'Andrea, A., Sander, C., and Ventura, A. (2009). Genetic dissection of the miR-17∼92 cluster of microRNAs in Myc-induced B-cell lymphomas. Genes Dev. *23*, 2806–2811.

26. Olive, V., Bennett, M.J., Walker, J.C., Ma, C., Jiang, I., Cordon-Cardo, C., Li, Q.J., Lowe, S.W., Hannon, G.J., and He, L. (2009). miR-19 is a key oncogenic component of mir-17-92. Genes Dev. *23*, 2839–2849.

27. Yan, H.J., Liu, W.S., Sun, W.H., Wu, J., Ji, M., Wang, Q., Zheng, X., Jiang, J.T., and Wu, C.P. (2012). miR-17-5p inhibitor enhances chemosensitivity to gemcitabine via upregulating Bim expression in pancreatic cancer cells. Dig. Dis. Sci. *57*, 3160–3167.

28. Guo, L., Xu, J., Qi, J., Zhang, L., Wang, J., Liang, J., Qian, N., Zhou, H., Wei, L., and Deng, L. (2013). MicroRNA-17-92a upregulation by estrogen leads to Bim targeting and inhibition of osteoblast apoptosis. J. Cell Sci. *126*, 978–988.

29. Grutzmacher, C., Park, S., Elmergreen, T.L., Tang, Y., Scheef, E.A., Sheibani, N., and Sorenson, C.M. (2010). Opposing effects of bim and bcl-2 on lung endothelial cell migration. Am. J. Physiol. Lung Cell Mol Physiol *299*, L607–L620.

30. Du, P., Wang, L., Sliz, P., and Gregory, R.I. (2015). A biogenesis step upstream of microprocessor controls miR-17-92 expression. Cell *162*, 885–899.

31. He, C., Gao, H., Fan, X., Wang, M., Liu, W., Huang, W., and Yang, Y. (2015). Identification of a novel miRNA-target gene regulatory network in osteosarcoma by integrating transcriptome analysis. Int. J. Clin. Exp. Pathol. *8*, 8348–8357.

32. Cerami, E., Gao, J., Dogrusoz, U., Gross, B.E., Sumer, S.O., Aksoy, B.A., Jacobsen, A., Byrne, C.J., Heuer, M.L., Larsson, E., et al. (2012). The cBio cancer genomics portal: an open platform for exploring multidimensional cancer genomics data. Cancer Discov. *2*, 401–404.

33. Fang, L.L., Wang, X.H., Sun, B.F., Zhang, X.D., Zhu, X.H., Yu, Z.J., and Luo, H. (2017). Expression, regulation and mechanism of action of the miR-17-92 cluster in tumor cells. (Review). Int. J. Mol. Med. *40*, 1624–1630.

34. Hesari, A., Azizian, M., Darabi, H., Nesaei, A., Hosseini, S.A., Salarinia, R., Motaghi, A.A., and Ghasemi, F. (2018). Expression of circulating miR-17, miR-25, and miR-133 in breast cancer patients. J. Cell Biochem. https://doi.org/10.1002/jcb.27984.

35. Li, H., Wu, Q., Li, T., Liu, C., Xue, L., Ding, J., Shi, Y., and Fan, D. (2017). The miR-17-92 cluster as a potential biomarker for the early diagnosis of gastric cancer: evidence and literature review. Oncotarget *8*, 45060–45071.

36. Northcott, P.A., Fernandez-L, A., Hagan, J.P., Ellison, D.W., Grajkowska, W., Gillespie, Y., Grundy, R., Van Meter, T., Rutka, J.T., Croce, C.M., et al. (2009). The miR-17/92 polycistron is up-regulated in sonic hedgehog-driven medulloblastomas and induced by N-myc in sonic hedgehog-treated cerebellar neural precursors. Cancer Res. *69*, 3249–3255.

37. Yamashita, A.S., Geraldo, M.V., Fuziwara, C.S., Kulcsar, M.A., Friguglietti, C.U., da Costa, R.B., Baia, G.S., and Kimura, E.T. (2013). Notch pathway is activated by MAPK signaling and influences papillary thyroid cancer proliferation. Transl Oncol. *6*, 197–205.